Predicting pK_a Using a Combination of Quantum Mechanical and Machine Learning Methods

Peter Hunt[1], Layla Hosseini-Gerami[2], Tomas Chrien[1], Jeffrey Plante[3], David J. Ponting[3], Matthew Segall[1]

[1] Optibrium Ltd, F5-6 Blenheim House, Cambridge Innovation Park, Denny End Road, Cambridge, CB25 9PB, UK Tel. +44 (0) 1223 815 900

[2] Department of Chemistry, Lensfield Road, Cambridge, CB2 1EW, UK Tel. +44 (0) 1223 336 300

[3] Lhasa Ltd, Granary Wharf House, 2 Canal Wharf, Leeds, LS11 5PS, UK Tel. +44 (0) 113 394 6020

Abstract

The acid dissociation constant (pK_a) has an important influence on molecular properties crucial to compound development in synthesis, formulation and optimisation of absorption, distribution, metabolism and excretion properties. We will present a method that combines quantum mechanical calculations, at a semi-empirical level of theory, with machine learning to accurately predict pK_a for a diverse range of mono- and polyprotic compounds. The resulting model has been tested on two external data sets, one specifically used to test pK_a prediction methods (SAMPL6) and the second covering known drugs containing basic functionalities. Both sets were predicted with excellent accuracy (root-mean-square errors of 0.7 – 1.0 log units), comparable to other methodologies using much higher level of theory and computational cost.

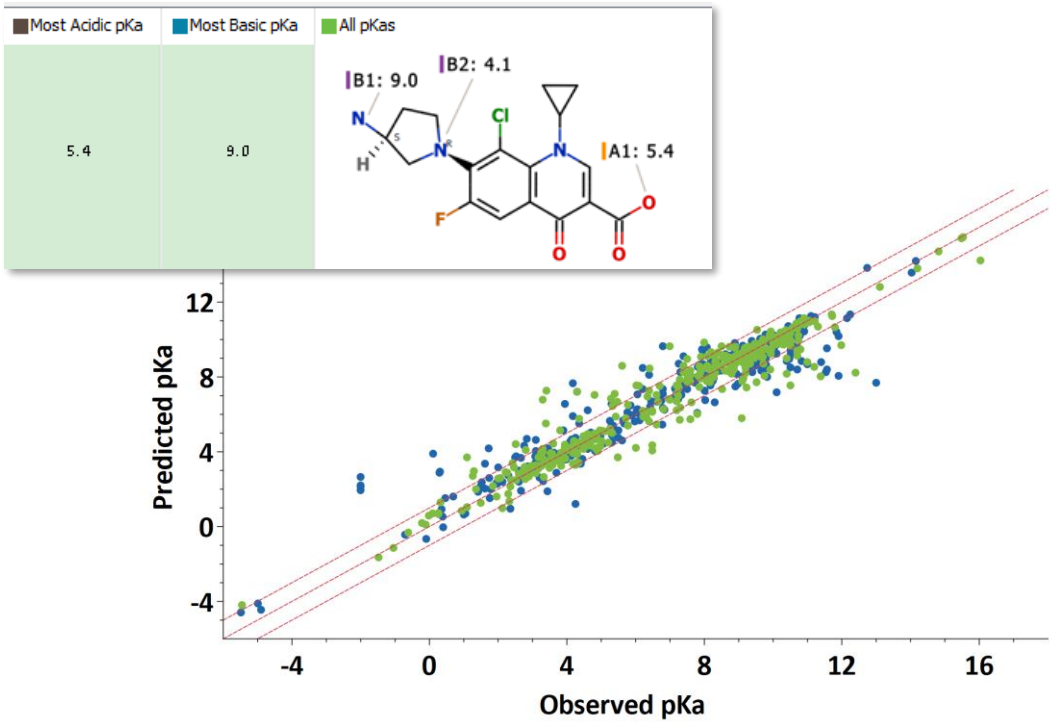

Introduction

The dissociation of a proton from a heteroatom has a significant influence on the charge distribution and interactions of a molecule. These influence many important molecular properties, including binding to target and off-target proteins, absorption, distribution, metabolism and excretion (ADME) and pharmacokinetic (PK) properties, such as solubility, tissue or cellular distribution and permeability. Therefore, the ability to predict the propensity of a molecule to lose or gain a proton in water is crucial for the development of new chemical entities with desirable PK, ADME and binding properties.

It is possible to model the free energy of the proton dissociation and gain very high accuracies using a quantum mechanical (QM) method based on density functional theory (DFT);[1,2] however these free energy relationships tend to be modelled on specific functional groups (carboxylic acids, anilines, phenols, etc.) and are applied to small data sets due to the computational cost of these high-level methods. Varekova *et al.* generated quantitative structure-activity relationship (QSAR) models on a set of phenols with partial charge descriptors for the Hydrogen, Oxygen and directly bonded Carbon atoms calculated using QM methods.[3] Their semi-empirical method using the Austin-Method 1 (AM1) Hamiltonian performed poorly, achieving a squared correlation coefficient (r^2) of only 0.45 and a root-mean-square error (RMSE) of 1.64; however the much more computationally expensive second-order Møller–Plesset (MP2) method with a 6-31G* basis set achieved an excellent r^2 of 0.97 and an RMSE of 0.40, albeit on a single class of ionizable sites. Harding and Popelier also investigated *ab initio* calculated descriptors for the prediction of pK_a for 171 phenols, this time considering bond length descriptors, with a similar r^2 of 0.92 and RMSE of 0.67.[4]

QSAR models have been built using other semi-empirical QM descriptors. Tehan *et al.* published two papers detailing a correlation with Fukui frontier molecular orbital (FMO) descriptors.[5,6] The authors looked at several different classes of protonation site, including phenols, carboxylic acids, amines and heterocycles, and used the AM1 method for all calculations. The r^2 coefficients for individual classes of site varied from 0.55 (heterocycles) to 0.94 (amines), with predictions improving with the addition of partial charge descriptors.

Several commercial vendors have developed pK_a models (ACDLabs,[7] SimulationsPlus,[8] Schrodinger,[9,10] ChemAxon,[11] Molecular Discovery[12]), which rely on linear free energy relationships (LFER) or QSAR methods and are derived from large databases of pK_a values (>10,000 data points in most cases). Liao and Nicklaus[13] compared nine different programs applied to the predicted pK_a values of 197 pharmaceutical compounds and found a range of performances (r^2 values from 0.58 to 0.94 and RMSEs from 1.8 to 0.65), where surprisingly the worst performing was a DFT-based method. However, it is very difficult to ascertain whether the more successful methods simply had more of the test compounds within their own training sets. Other reviews of pK_a tools have been published, at least in part, based on proprietary compounds Balogh *et al.* published results on their in-house dataset of 95 compounds, [14] Manchester *et al.* evaluated the predictive performance on 211 drug-like compounds,[15] Settimo *et al.* from Vertex used datasets of in-house and external sources to show how varied the performance can be between models.[16] The success of each method depended on the test dataset used and on the ability of each model to recognise potential ionisable sites. Hence, the performance varied depending on the ionisable site considered (bases tended to be less well predicted compared to acids).

Our aim was to create a model using a semi-empirical QM approach combined with machine learning. We wished to retain the physically relevant contributions to the electrostatics, provided by consideration of the whole molecular environment, while balancing this with acceptable computational cost and speed of calculation. The model we describe herein employs a single model (not specific to any ionisable group), derived from a comparatively small, but carefully curated data set of aqueous pK_a values for mono- and diprotic compounds, where the atomic assignment of pK_a values to specific heteroatoms or groups was unambiguous. This is essential for a correct characterisation of the ionised site to reduce the potential for noise in the data, where the association of a pK_a with an exact site can be lost in databases containing very large numbers of polyprotic molecules.

Methods

Data Set

A data set was collated from public data sources[17,18,19] and comprises aqueous pK_a determinations at temperatures close to 25 degrees. Each data point was carefully inspected to ensure that the assignment of the pK_a value to a specific site or group was clear and unambiguous.

The total data set contained 2,435 pK_a values, which were split into 1,722 values in the training set, 359 in the validation set and 354 in the test set. These corresponded to 2,243 unique compounds of which 1,570 were in the training set, 336 in the validation set and 337 in the test set (a split equivalent to 70%:15%:15% of the compounds created by random selection). The purpose of the validation and test sets are to provide two independent assessments of any model generated, the validation set allows the selection of the best performing methodology and the test set is a check to ensure that this selection has not been influenced by random chance. Valid models should perform equally well on both sets whilst a much poorer performance on the test set would indicate a biased model or simply a good validation result by random chance.

Simple property distributions for these sets are shown in Figure 1 and one can see that the molecules included are distributed more towards the smaller, less functionalised end of the property ranges. However, this is in keeping with the dataset construction strategy to include only molecules with unambiguous assignment of pK_a values to atomic sites. Despite this, there are representative 'drug like' molecules included in the training, validation and test sets.

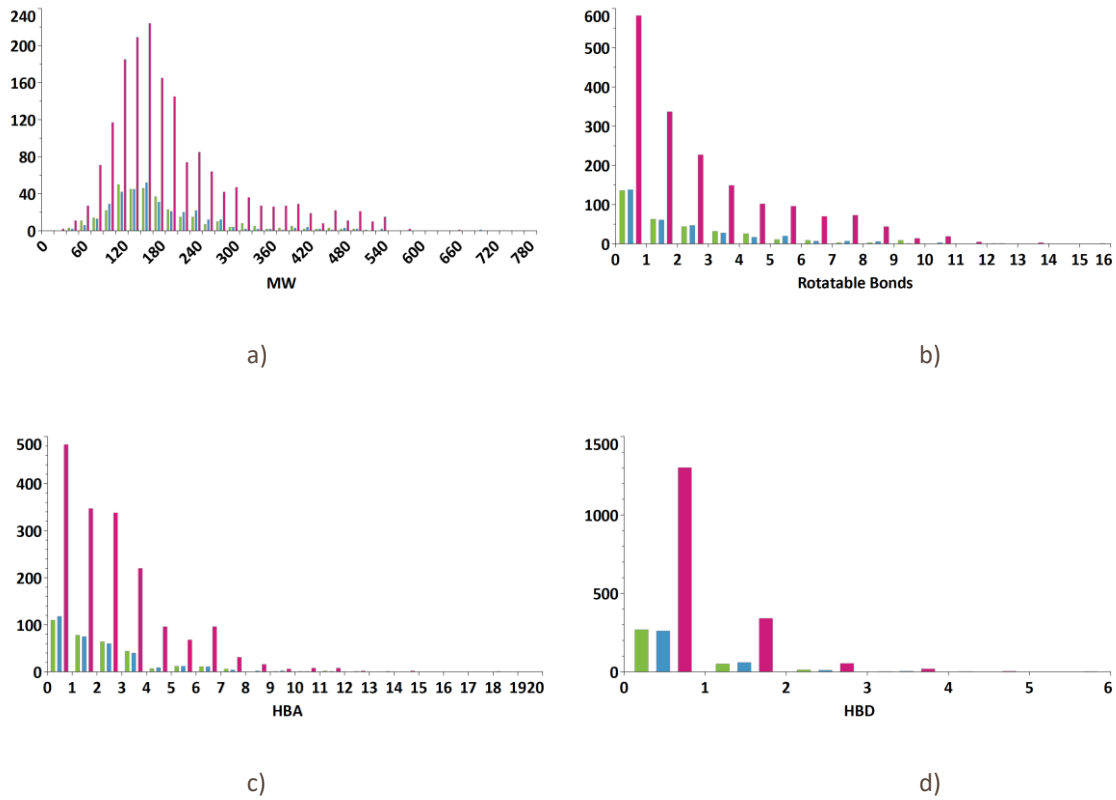

Figure 1. Plots of the distributions of simple properties across the training (red bars), validation (blue bars) and test (green bars) sets. a) Molecular weight, b) Rotatable bonds, c) Hydrogen bond acceptors, d) Hydrogen bond donors.

Descriptor Calculation

A single 3-dimensional conformation was generated for each compound using OMEGA.[20] If stereochemistry was defined in the SMILES then this was maintained in the 3D structure, but if no stereochemistry was defined then a single stereochemical configuration was taken from OMEGA.

The parent and subsequent structures were optimised using the AM1 Hamiltonian in MOPAC[21] with the following keywords "AM1 EF PRECISE MMOK VECTORS T=3600 CYCLES=1000 EIG-EXOUT GEO-OK CHARGE=*" where the charge keyword value '*' was set appropriately for the compound charge state.

Hydrogen atoms were then added or removed from the parent structure to create the appropriate conjugate acid or conjugate base and the Hydrogen atom positions were adjusted as required using OMEGA. This newly ionised structure was again optimised through MOPAC and the descriptor calculation repeated. The descriptors used capture atomic and bond properties, describing the Hydrogen, heteroatom (X) and all of the heavy atom neighbours (R) of the heteroatom in the conjugate acid and base forms for the ionisable site, as illustrated in **Figure 2**. Nucleophilic and electrophilic delocalisabilities, bond lengths and atom charge descriptors were calculated for the heteroatom and nearest heavy-atom neighbours. Each of the descriptors calculated for the individual heavy atoms, R, were averaged across the n heavy atoms' neighbours to produce a single value. The HOMO and LUMO energies and heats of formation of the conjugate acid and base were also used as descriptors.

Figure 2. The atoms considered in the parameterisation of the model where 'n' refers to all the directly bonded heavy atoms of the heteroatom X.

This process was repeated for each site considered as likely to be ionised in a reasonable pK_a range. Currently alkyl or unsubstituted amide and sulphonamide NH groups and Carbons are excluded; however, these could be introduced by the inclusion of accurate pK_a determinations to the training set. For polyprotic compounds, each site was protonated or deprotonated individually and the most basic and/or most acidic site was identified. A second round of calculations was then performed where this primary site was ionised and the other sites were examined to determine the second-most basic/acidic site; if the molecule was zwitterionic, the process was repeated with the other acidic/basic site charged as this enables a better prediction for the most acidic/basic sites. Once these two most acidic/basic sites were determined, a final round of calculations were performed for any other isonisable site, with these two sites in their appropriate charge states. These heuristics provide a way of capturing the effect of ionisation of the most acidic and basic sites in a molecule on the estimation of the acidity/basicity of subsequent sites.

We are not attempting to explicitly calculate specific micro pK_a states of a molecule, with appropriate Boltzmann-weighted contributions for each state, as this extends the calculation time and provided little gain in accuracy. Our aim, with these heuristics, is to produce a set of predictions that are more realistic evaluations of the charge state of a molecule in water and, as such, the ease or otherwise of introducing a second or subsequent charged site into a system that already bears a charge (or charges) should be considered and predicted appropriately.

Model Generation

Models were generated and tested using the data set and descriptors described above, employing three methods implemented in the Auto-Modeller™ module of the StarDrop™ software[22]: a linear method, partial least square (PLS);[23] radial basis functions (RBF);[24] random forests (RF);[25] and Gaussian processes (GP) with conjugate gradient optimisation of hyperparameters.[26]

RBFs have been praised for their simplicity, robustness and ease of implementation in multivariate scattered data approximation. Such techniques have been applied with success in problems ranging from training neural networks to image compression.[24] A radial basis function is a non-linear transfer function which aims to approximate a real valued function where the Euclidean distance between the points in descriptor space is minimised. In the training step the function passes through every training point and the weights for each row function solved to produce the final fitted function used to predict test points. The functional form used can vary (including linear, cubic, multi-quadratic and Gaussian) but the methodology used herein uses a linear function.

Results & Discussion

The results for the three methods applied to the independent validation and test sets are summarised in Table 1, which shows the coefficient of determination (R^2), RMSE and Mean Absolute Deviation (MAD) for each model.

The best performing model was derived using the Radial Basis Function methodology the results on the independent validation and test sets are shown in Figure 3. The remaining analyses, described below, relate to this model. Please note that in cases where multiple potential sites of ionisation are present in the same functionality and a clear assignment cannot be made, e.g. a piperazine, both were included in the validation and test sets and hence the associated error represents an average between these to give a fair assessment. However, including only the closest agreement between the model predictions and the experimental value only reduced the RMSE values by around 0.02 in the test set and 0.07 in the validation set.

Table 1. The performance of the models for the independent validation and test sets. The coefficient of determination (R^2) root-mean-square error (RMSE) and mean absolute deviation (MAD) is shown for each set. GP is Gaussian processes, RBF is radial basis function, RF is random forests, PLS is partial least squares.

Method	Validation Set			Test Set		
	R^2	RMSE	MAD	R^2	RMSE	MAD
RBF	0.90	1.05	0.65	0.92	0.91	0.59
GP	0.86	1.28	0.84	0.85	1.21	0.80
RF	0.87	1.25	0.82	0.88	1.12	0.74
PLS	0.66	2.0	1.43	0.69	1.81	1.32

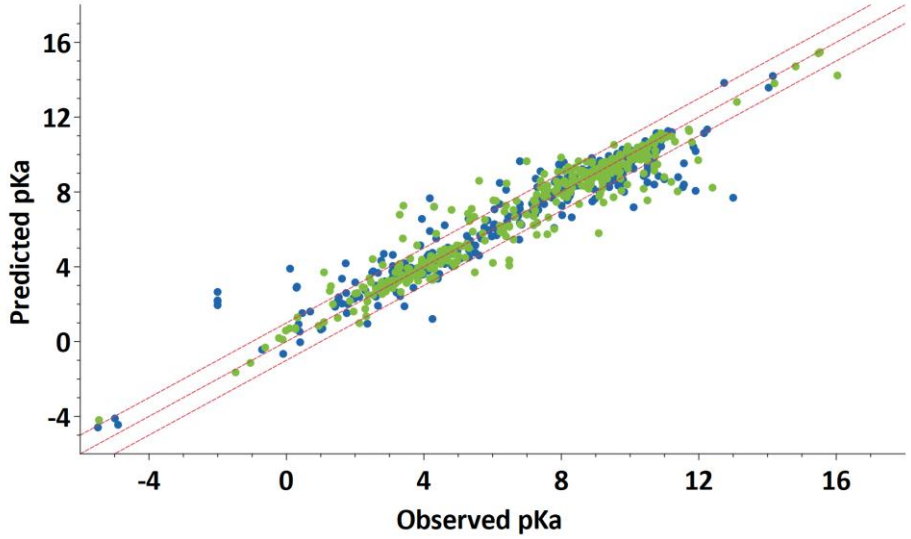

Figure 3. A plot of predicted versus observed pK_a values for the validation (blue points) and test (green points) sets. The identity line and lines deviating by ±1 log unit are shown as red dotted lines.

An alternative view of the model performance is to analyse the error distribution, as RMSE values can be influenced by a small number of large outliers. For the validation and test sets 34% and 32% of the pK_a values are predicted within 0.2 log units; this rises to 68% for the validation and 69% for the test set within 0.6 log units and 79% and 83% within 1 log unit respectively. 90% of the validation set has a deviation below 1.6 whilst for the test set this deviation is only 1.46 log units.

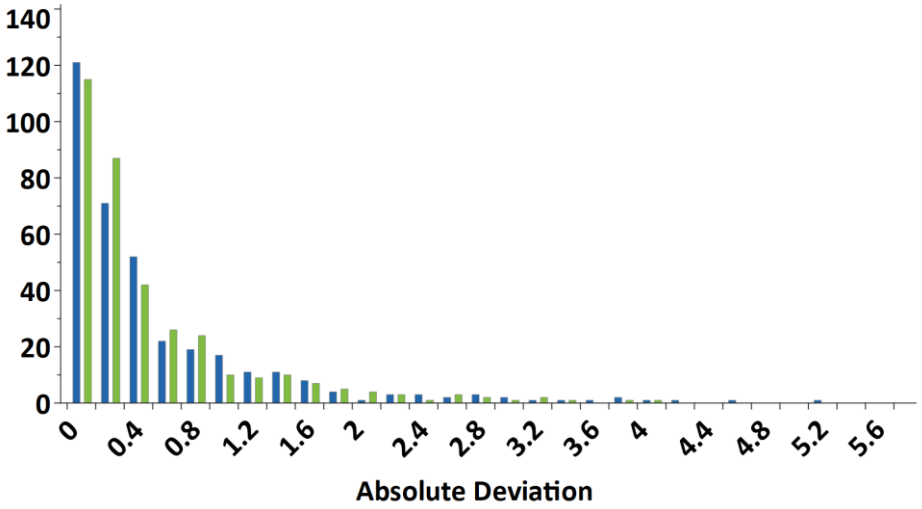

Figure 4. A plot of absolute deviations for the validation (blue bars) and test (green bars) sets. The largest deviations were found to occur for some of the extreme measured pK_a values.

The distribution of deviations is very similar for both acidic and basic pK_a values, as shown in Figure 5, although it is interesting to see the higher proportion of small deviations in the acid predictions in the test set relative to the validation set.

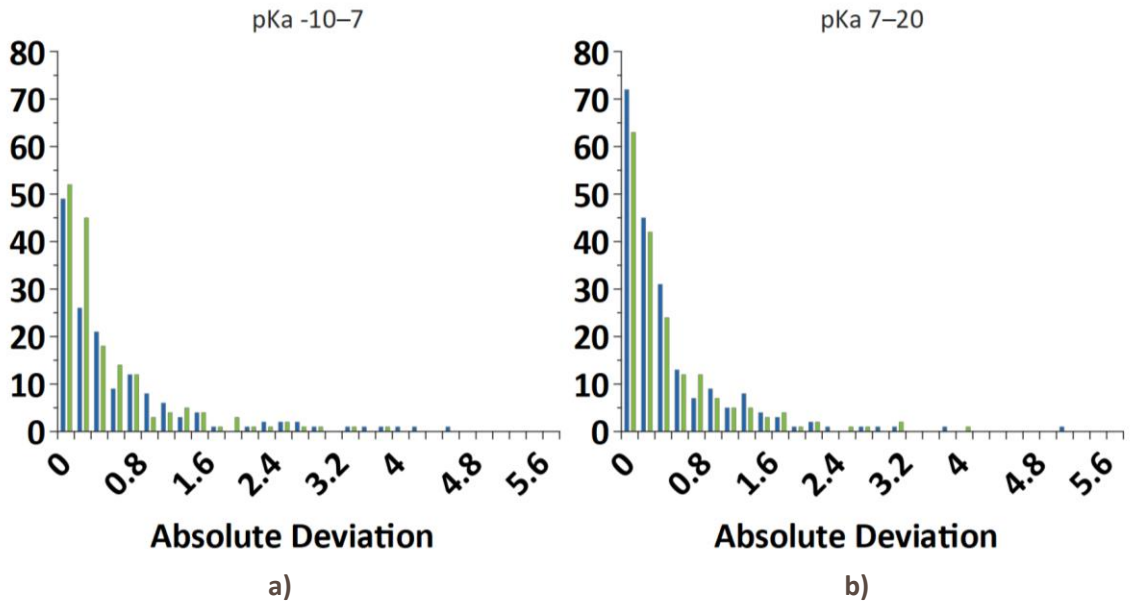

Figure 5. A plot of absolute deviations for the validation (blue bars) and test (green bars) sets for acidic and basic experimental pK_a values (a) is $pK_a \leq 7$, b) is $pK_a > 7$).

The speed of the predictions is of interest in the application of this methodology to drug design. The submission of the validation and test sets to the model, without prior calculation of the descriptors, resulted in average calculation times per molecule of 17 and 20 seconds respectively on a single threaded CPU (Intel® i7-8550U @ 1.8GHz). Parallelisation of this methodology is eminently feasible and would enable even large collections of molecules to be predicted in a reasonable timeframe.

Comparison on Benchmarking Data Sets

This model was further validated by testing against two published data sets. The SAMPL6 data set comprises 24 kinase inhibitor-like molecules with 31 experimental pK_a values and was specifically devised to test pK_a prediction methods.[27] The second was a set of 48 amine-containing drug molecules (53 pK_a values) devised by Jensen *et al.*[28], which had been used to evaluate semi-empirical pK_a prediction methodologies, similar to that used in this paper.

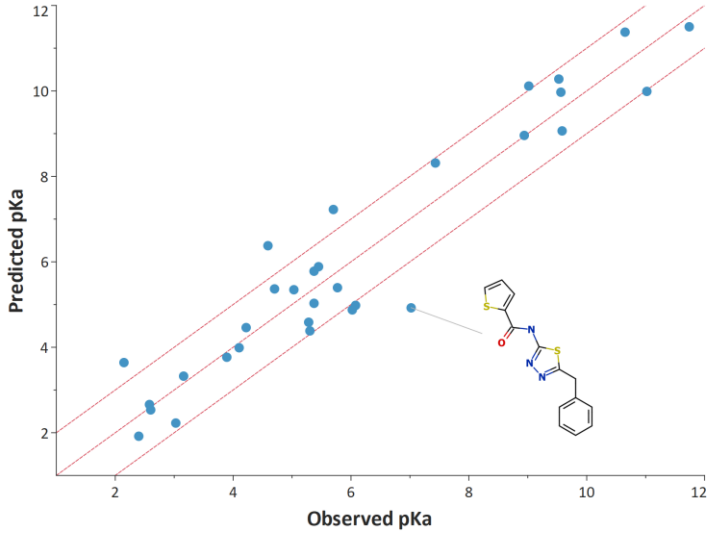

Figure 6. Plot of predicted versus observed pK_a values for the SAMPL6 data set. The identity line and lines deviating by ±1 log unit are shown as red dotted lines, the compound with the largest misprediction is shown.

The RMSE on the whole SAMPL6 set was 0.85 and the predicted versus observed graph is shown in Figure . This compares very favourably with the published performances of the other methods shown in Table 1, where the authors noted that some outliers were removed due to sites not being thought of as ionisable or extra modifications were required such as conformational sampling. The only method to achieve a better RMSE than the model herein is that published by Pracht *et al.* which uses a very computationally expensive LFER method based on DFT with conformational sampling.[2] Note that none of the compounds from this data set were included in the training or validation sets for the models described herein, so this represents a fair comparison.

Table 1. Summary of the performance of published methods on the SAMPL6 benchmarking data set. The, method, root-mean-square error (RMSE) and comments made by the authors in the corresponding references are shown.

Author	Method	RMSE	Comments
Bannan *et al.*[29]	Gaussian process model	2.2	reducing to 1.7 by removing an outlier SM06 – an amide anion
Pracht *et al.*[2]	LFER with conf. sampling and DFT	0.68	
Prasad *et al.*[30]	Hybrid QM/MM with explicit solvent	2.4	"protocol needs work"
Selwa *et al.*[31]	*ab initio* QM free energies	1.95	
Tielker *et al.*[32]	EC-RISM	1.7	reducing to 1.5 with improved electrostatics and 1.1 with conf. sampling
Zeng *et al.*[33]	M06-2X DFT with SMD solvation model	1.4	falling to 0.73 with linear correction

The results obtained for the set published by Jensen *et al.*[28] are complicated by the presence of some of the compounds from this set in the training set of our model. However, the RMSE for the prediction of all of the pK_a values within the set is 0.98, which rises only slightly to 1.05 for the 45 pK_a values not included in our training set. These results are equivalent to those obtained by Jensen *et al.* with solvent corrected values using COSMO and either the PM3 or AM1 semi-empirical methods, but only when the zwitterion Cefadroxil is excluded from their analysis.

A graph of predicted versus observed pK_a is shown for the Jensen *et al.*[28] data set in Figure (a), in which some of the outlier compounds are highlighted. These compounds indicate where our methodology might be improved either by additional data, or by the higher computational cost incurred by conformational sampling. The amidine Phenacaine highlights the relative paucity of acyclic amidines in our training set, whilst the Sparteine structure highlights the stabilisation of a protonated structure through internal Hydrogen bonding. Our procedure essentially describes the equilibrium between the Hydrogen on the ionisable compound and water, whereas the environment of the Hydrogen in Sparteine is influenced by the other Nitrogen within the Sparteine molecule (as shown in Figure (b)). Hence the specific Nitrogen-Hydrogen environment evaluated in our calculations gives rise to a less basic prediction than observed experimentally, as the internal H-bond is not captured by molecules in our training set and we only consider one conformation of the training and test molecules. The other outliers at the bottom left are the second pK_a (i.e. the di-protonated pK_a) values quoted for Hydroquinine and Procaine respectively; the monoprotonated values are predicted within 1 log unit error.

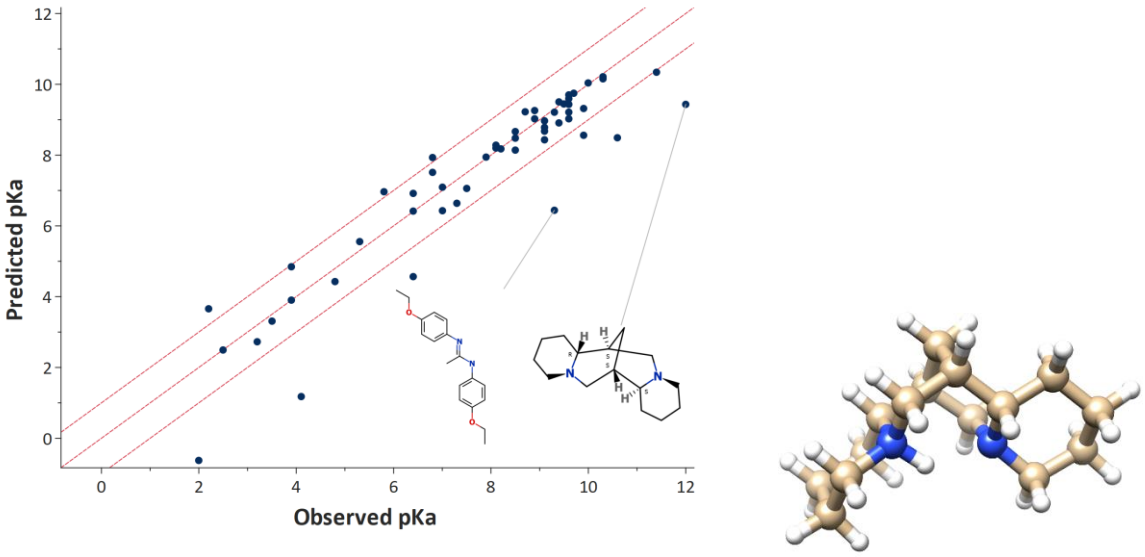

Figure 7. (a) Plot of predicted versus observed pK_a for the data set published by Jensen et al.[28] The identity line and lines deviating by ±1 log unit are shown as red dotted lines. Two main outliers, Sparteine and Phenacaine are highlighted the other main outliers are secondary rather than primary pk_a values. (b) a 3-dimensional conformation of Sparteine illustrating the interaction between the proton and two Nitrogens that is not accurately captured by the model, giving rise to an inaccurate prediction.

Conclusion

We have described a method combining semi-empirical QM and machine learning methodologies for the prediction of pK_a for both mono- and poly-protic species. This gives rise to a single model that can be applied reliably across acidic and basic functionalities. The model performs as well as more computationally intensive methods on two published test sets, which were devised to specifically benchmark pK_a prediction methods and cover important areas of drug-like molecules. Our methodology considers the effects of the whole molecule on the immediate vicinity of the ionisable site and therefore incorporates more information about the molecular environment than is considered in simple isolated fragment-based QSAR methodologies. The speed of our method is still more than acceptable for the calculation of many hundreds of molecules encountered in a drug design or agrochemical optimisation process.

References

1. Zhang, S.; Baker, J.; Pulay, P. A Reliable and Efficient First Principles-Based Method for Predicting pK_a Values. 1. Methodology, *J. Phys. Chem. A* **2010,** *114* (1), pp. 425-431.
2. Pracht, P.; Wilcken, R.; Udvarhelyi, A.; Rodde, S.; Grimme, S. High accuracy quantum‐chemistry‐based calculation and blind prediction of macroscopic pK_a values in the context of the SAMPL6 challenge *J. Comp.-Aid. Mol. Des*. **2018,** *32*, 1139–1149.
3. Svobodová Vařeková, R.; Geidl, S.; Ionescu, C.; Skřehota, O.; Kudera, M.; Sehnal, D.; Bouchal, T.; Abagyan, R.; Huber, H.; Koča, J. Predicting pK_a Values of Substituted Phenols from Atomic Charges: Comparison of Different Quantum Mechanical Methods and Charge Distribution Schemes *J. Chem. Inf. Model.* **2011,** *51* (8), 1795-1806.
4. Harding, A.; Popelier, P. pK_a Prediction from an ab initio bond length: part 2—phenols *Phys. Chem. Chem. Phys.* **2011,** *13* (23), 11264.
5. Tehan, B.; Lloyd, E.; Wong, M.; Pitt, W.; Montana, J.; Manallack, D.; Gancia, E. Estimation of pK_a Using Semiempirical Molecular Orbital Methods. Part 1: Application to Phenols and Carboxylic Acids *Quantitative Structure-Activity Relationships*, **2002,** *21* (5), 457-472.
6. Tehan, B.; Lloyd, E.; Wong, M.; Pitt, W.; Manallack, D.; Gancia, E. Estimation of pK_a Using Semiempirical Molecular Orbital Methods. Part 2: Application to Amines, Anilines and Various Nitrogen Containing Heterocyclic Compounds *Quantitative Structure-Activity Relationships*, **2002,** *21* (5), 473-485.
7. ACD/pKa :: Predict accurate acid/base dissociation constants from structure :: ACD/Labs Percepta Predictors, *Acdlabs.com*, 2017. [Online]. Available: http://www.acdlabs.com/products/percepta/predictors/pka/ Last accessed: 10th Oct. 2019.
8. Fraczkiewicz, R.; Lobell, M.; Göller, A.; Krenz, U.; Schoenneis, R.; Clark, R.; Hillisch, A. Best of Both Worlds: Combining Pharma Data and State of the Art Modeling Technology To Improve in Silico pK_a Prediction *J. Chem. Inf. and Model.* **2015,** *55*, (2), 389-397. [Online]. Available: https://www.simulations-plus.com/software/admetpredictor Last accessed: 10th Oct. 2019.
9. Shelley, J.; Cholleti, A.; Frye, L.; Greenwood, J.; Timlin, M.; Uchimaya, M. Epik: a software program for pK_a prediction and protonation state generation for drug-like molecules *J. Comp.-Aid. Mol. Des.* **2007,** *21*, (12), 681-691.
10. Klicić, J.; Friesner, R.; Liu, S.; Guida, W. Accurate Prediction of Acidity Constants in Aqueous Solution via Density Functional Theory and Self-Consistent Reaction Field Methods *J. Phys. Chem. A* **2002,** *106*, (7), 1327-1335.
11. pKalc. [Online]. Available: http://www.compudrug.com/pkalc. Last accessed 10th Oct. 2019.
12. Milletti, F.; Storchi, L.; Sforna, G.; Cruciani, G. New and Original pK_a Prediction Method Using Grid Molecular Interaction Fields *J. Chem. Inf. Model.* **2007,** *47*, (6), 2172-2181. MoKa from Molecular Discovery https://www.moldiscovery.com/software/moka/ last accessed 10th Oct. 2019.
13. Liao, C.; Nicklaus, M. Comparison of Nine Programs Predicting pK_a Values of Pharmaceutical Substances *J. Chem. Inf. Model.* **2009,** *49*, (12), 2801-2812.

14. Balogh, G. T.; Tarcsay, A.; Keseru, G. M. Comparative evaluation of pK_a prediction tools on a drug discovery dataset, *J. Pharm. Biomed. Anal.* **2012,** *67-68,* 63-70.
15. Manchester, J.; Walkup, G.; Rivin, O.; You, Z. Evaluation of pK_a Estimation Methods on 211 Druglike Compounds *J. Chem. Inf. Model.* **2010,** *50*, (4), 565-571.
16. Settimo, L.; Bellman, K.; Knegtel, R. Comparison of the Accuracy of Experimental and Predicted pKa Values of Basic and Acidic Compounds *Pharm. Res.* **2013,** *31*, (4), 1082-1095.
17. Gaulton, A.; Bellis, L. J.; Bento, A. P.; Chambers, J.; Davies, M.; Hersey, A.; Light, Y.; McGlinchey, S.; Michalovich, D.; Al-Lazikani, B.; Overington, J. P. ChEMBL: a large-scale bioactivity database for drug discovery. *Nucleic Acids Res.* **2012,** *40*, D1100-7.
18. Dissociation constants of organic bases in aqueous solution Perrin, D. D. London : Butterworths, 1965 and 1972
19. Dissociation constants of organic acids in aqueous solution Kortüm, G.; Vogel, W.; Andrussow, K. London : Butterworths, 1961.
20. Hawkins, P.C.D.; Skillman, A.G.; Warren, G.L.; Ellingson, B.A.; Stahl, M.T. Conformer Generation with OMEGA: Algorithm and Validation Using High Quality Structures from the Protein Databank and Cambridge Structural Database, *J. Chem. Inf. Model*. **2010**, *50*, 572-584. https://www.eyesopen.com/omega last accessed 10th Oct. 2019.
21. Stewart, J. J. P. MOPAC: A General Molecular Orbital Package, *Quant. Chem. Prog. Exch*., **1990,** *10*, 86.
22. StarDrop https://www.optibrium.com/stardrop last accessed 10th Oct. 2019.
23. Wold, S.; Sjöström, M.; Eriksson, L. Partial Least Squares Projections to Latent Structures (PLS) in Chemistry. Encyclopedia of Computational Chemistry; Schleyer, P. v. R.; Allinger, N. L.; Clark, T.; Gasteiger, J.; Kollman, P.; Schaefer, H. F. III; Schreiner, P. R. Eds.; Wiley: Chichester, U. K., **1998,** *3*, 2006-2022.
24. Radial Basis Functions Buhmann, M. D., Cambridge University Press, 2003 ISBN: 9780511543241, https://doi.org/10.1017/CBO9780511543241
25. Breiman, L. Random Forests, *Machine Learning*, **2001,** *45*(1), 5-32.
26. Obrezanova, O.; Csanyi, G.; Gola, J. M. R.; Segall, M. D. Gaussian Processes: A Method for Automatic QSAR Modelling of ADME Properties *J. Chem. Inf. Model*. **2007,** *47*(5), 1847-1857.
27. Isik, M.; Levorse, D.; Rustenburg, A. S.; Ndukwe, I. E.; Wang, H.; Wang, X.; Reibarkh, M.; Martin, G. E.; Makarov, A. A.; Mobley, D. L.; Rhodes, T.; Chodera, J. D. pK_a measurements for the SAMPL6 prediction challenge for a set of kinase inhibitor-like fragments *J. Comp.-Aid. Mol. Des*. **2018,** *32*, 1117-1138.
28. Jensen, J. H.; Swain, C. J.; Olsen, L. Prediction of pKa values for druglike molecules using semiempirical quantum chemical methods *J. Phys. Chem. A* **2017,** *121*, (3), 699-707.
29. Bannan, C. C.; Mobley, D. L.; Skillman, A. G. SAMPL6 challenge results from pK_a predictions based on a general Gaussian process model *J. Comp.-Aid. Mol. Des*. **2018,** *32*, 1165–1177.
30. Prasad, S.; Huang, J.; Zeng, Q.; Brooks, B. R. An explicit‐solvent hybrid QM and MM approach for predicting pK_a of small molecules in SAMPL6 challenge *J. Comp.-Aid. Mol. Des*. **2018,** *32*, 1191–1201.
31. Selwa, E.; Kenney, I. M.; Beckstein, O.; Iorga, B. I. SAMPL6: calculation of macroscopic pK_a values from *ab initio* quantum mechanical free energies *J. Comp.-Aid. Mol. Des*. **2018,** *32*, 1203–1216.
32. Tielker, N.; Eberlein, L.; Güssregen, S.; Kast, S. M. The SAMPL6 challenge on predicting aqueous pK_a values from ECRISM theory *J. Comp.-Aid. Mol. Des*. **2018,** *32*, 1151–1163.
33. Zeng, Q.; Jones, M. R.; Brooks, B. R. Absolute and relative pK_a predictions via a DFT approach applied to the SAMPL6 blind challenge *J. Comp.-Aid. Mol. Des*. **2018,** *32*, 1179–1189.